# HIGH PRESSURE MELT EJECTION RELEVANT TO CANDU REACTORS

**N.N.Wahba and M.H.Bayoumi**

**Ontario Hydro Nuclear, Fuel and Fuel Channel Analysis Department**
**700 University Avenue, Toronto, Ontario, M5G-1X6**

ABSTRACT

The modelling of fuel-coolant interaction following a severe flow blockage in a single channel of a CANDU reactor is assessed. The available data that support these models is also reviewed. It is concluded that it is appropriate to employ the forced fuel-coolant interaction methodology in analyzing CANDU single channel flow blockage event with a severe power-cooling mismatch. The hydrodynamic transients are conservatively determined for various amounts of molten fuel available for discharge. The magnitude of the pressure transient and impulse loads decrease as the distance from the rupture site increases. The higher discharged mass produces more energy deposited in the bubble over the transient which results in a faster and greater pressurization of the moderator and results in higher impulsive loads on adjacent structures.

## 1.0 INTRODUCTION

The core of a CANDU reactor includes a large number of fuel channels connected by feeder pipes to common headers. Each channel thus represents a discrete flow path in a complex network of parallel pipes. The thermal conditions in each of these channels are governed by local parameters (mainly the channel power and coolant flow).

In case of a severe flow blockage by an undetected obstruction in the coolant flow path somewhere between the inlet and outlet feeder connections to the headers, the reduction in the coolant flow rate through the affected channel while the fuel still operates at its full power may develop a mismatch between the power generation in the channel and the heat capability of the coolant.

There are three possible channel responses to a severe power/cooling mismatch at full reactor power and high heat transport system pressure following a blockage of primary heat transport coolant flow in a single fuel channel. When a sufficient convective heat removal is available to avoid pressure tube ballooning, there is no channel failure, and fuel temperatures remain relatively low. During ballooning at high pressure, any small temperature gradients invariably induce pressure tube failure. When the fuel channel fails early during pressure tube ballooning, there is either no molten material in the channel at the time of failure, or any small amount of melt generated is confined within the fuel elements. If the pressure tube balloons uniformly into contact with its calandria tube, some fuel liquefaction occurs, and channel failure is induced by the relocation of melt from the fuel bundle interior to the composite wall of the ballooned channel. However, all ballooning experiments relevant to CANDU reactor at full system pressure (10 MPa) resulted in pressure tube failure prior to contact with calandria tube.

Although the last type of channel response is highly unlikely, its consequences are more severe than the other types since it may lead to energetic Fuel-Coolant Interactions (FCIs). The hydrodynamic transients following a postulated rupture of a pressure tube and the associated calandria tube may cause damage to the

adjacent structures such as neighbouring channel, shut off rods guide tubes and the calandria vessel. The potential damage depends on the transient pressure field within the calandria vessel.

Two analysis methodologies are available for the modelling of fuel-coolant interactions following a severe power-cooling mismatch in a single channel of a CANDU reactor. The two methodologies address different physical phenomena. The first model postulates that the melt is ejected from the channel at sufficiently high velocities to be finely fragmented and rapidly quenched within milliseconds of the ejection. This model is called forced interaction model. The second model postulates that the ejected melt first accumulates outside of the channel as a coarse melt-water-steam mixture. Some time later, this coarse mixture is triggered to finely fragment and rapidly quench. This model is called free interaction model.

Reference [1] examined the consequences of a pressurized melt ejection into the calandria vessel assuming a large fraction of molten fuel present at the time of rupture to be employed to calculate an upper bound of flow blockage consequences. A model was formulated to quantify the pressure loads generated by the forced fuel-coolant interactions in CANDU calandria vessels [1]. This model computes the highly transient melt ejection rates, and it assumes that the ejected melt is finely fragmented such that the molten droplets rapidly transfer all their heat to the surrounding liquid. During the forced FCI, the melt is finely fragmented and dispersed not only by the contact with water, but also by the shattering of melt droplets when they impact on near-by structures and/or the calandria vessel floor.

This paper examines the modelling of potential energetic fuel-coolant interactions following a severe power-cooling mismatch in a single fuel channel of a CANDU reactor. The experimental programs relevant to CANDU reactors are summarized in section 2. The analytical model and results are described in sections 3 and 4, respectively. Conclusion remarks are given in section 5.

## 2.0 EXPERIMENTAL PROGRAMS OF HIGH PRESSURE MELT EJECTION

A number of experimental studies have been performed to investigate the process and behaviour of pressurized melt ejection. These programs are summarized in this section. The experiments may be divided into three categories, namely, Direct Containment Heating (DCH), Reactivity Initiated Accident (RIA), and in-core damage experiments.

### 2.1 Direct Containment Heating (DCH) Experiments

In the DCH process, it is considered that the melt accumulates in the lower head of a Pressurized Water Reactor (PWR) pressure vessel under high pressure coolant conditions. Failure of the vessel at a location in contact with the melt would then lead to gas-pressure-driven ejection of melt into the reactor cavity region and eventual deposition of the melt onto the floor of the containment building. Because of the presence of water in the reactor cavity region, a molten fuel-coolant interaction may occur. The concern related to the high-velocity melt discharge is usually with a direct containment heating (DCH) of the containment atmosphere by the finely fragmented melt droplets.

The DCH experiments include: Corium-Water Thermal Interaction Experiments (CWTI) [2], System Pressure Injection Tests (SPIT) [2,3,], High Pressure Melt Streaming Series (HIPS) [2,3], Limited Flight Path Experiments (LFP) [4], Wet Cavity Experiments (WC) [5], and Integral Effects Tests (IET) [6]. In some of these experiments, molten material was ejected by high pressure steam into a cavity having no, or little water (condensate levels of water). In other experiments, with water in the cavity [3], energetic fuel-

coolant interactions that destroyed the cavity were observed. Due to early failure, little data was recorded in these experiments. Other experiments with a robust cavity, designed to withstand large loads, are considered more reliable and relevant to CANDU reactors.

The DCH experimental results suggest that the high-velocity molten jet from the reactor vessel is fragmented while moving to the base of the cavity under the influence of a high velocity and perhaps dissolved gas release [2]. High pressure gases in the reactor pressure vessel (steam and hydrogen), that follow the melt from the vessel, flow at high velocity through the cavity, and fragment the melt into smaller particles. These particles are created from the melt by a combination of several mechanisms: melt jet breakup by the action of gases, atomization, entrainment process and Weber breakup. In some experiments, an energetic melt-water interaction invariably commenced when the molten jet fragmented and dispersed by impacting the cavity floor. This experimental series is relevant to the CANDU single channel events in demonstrating the effectiveness of mechanical melt fragmentation due to impact on the adjacent in-core structures.

Four Integral Effects Tests (IET-1, IET-7, IET-8A and IET-8B) were conducted to investigate the effects of FCI on DCH [6]. The relevant initial conditions of these tests are listed in Table 1. The cavity pressures measured in the experiments are shown in Figure 1 (taken from Reference [6]). The results indicate that energetic FCI occurred when the cavity half-filled with water as shown for tests IET-8A and IET-8B, whereas the interactions appeared to be the result of rapid vaporization of the small amount of water in the cavity as shown in test IET-7. The results of test IET-8B indicate that when the molten material was ejected by relatively high pressure into the cavity (about 6.25 MPa), FCI began immediately after the initiation of the high pressure melt ejection (at time 0.0 sec) and continued throughout the blowdown of the melt. The results of this test displayed the shape of the hydrodynamic transient characterized by forced interaction (*i.e.*, a pressure transient occurring immediately after the rupture). Test IET-8B yielded the highest integrated pressure recorded in the test series. However, in the similar experiment IET-8A, where the molten material was essentially dropped into the cavity, a delayed FCI occurred near the end of the molten pour into the cavity (at time 0.25 sec) resulting in a larger and shorter in duration pressure spike displaying the shape of the hydrodynamic transient characterized by free interaction.

## 2.2 Reactivity Initiated Accident (RIA) Experiments

Experiments were performed in Japan by JAERI [7] to investigate fuel-coolant interactions during reactivity initiated accidents. These experiments have initial conditions similar to those postulated in a CANDU channel in terms of the high driving pressure, the simultaneous presence of molten and solid $UO_2$ at the time of rupture, and the rapid rupture opening to a limited length. The initial pressures ranged from ambient to 8 MPa. The results of these tests displayed the shape of the hydrodynamic transient characterized by forced interaction (*i.e.*, a pressure transient occurring immediately after the rupture). Furthermore, the magnitude of the pressure spike was observed to increase as the driving pressure increases, which is consistent with the finer melt fragmentation that occurs as the melt velocities increase.

In some of the Japanese tests, secondary pressure excursions occurred 5 to 10 ms after the first pressure peak. However, it appears that the experiments, which experienced the secondary fuel-coolant interactions, actually involved low-velocity melt pours in the later stages of tests (*i.e.*, the transient melt generation continued after the fuel element had depressurized). Considering the fuel enthalpy at cladding failure relative to the total energy deposition into the fuel during those tests, any appreciable secondary pressure excursion occurred only when the melt continued to be generated after the cladding has ruptured.

## 2.3 In-Core Damage Experiments

One experimental test series has been conducted by Isles [8], which represents conditions similar to that postulated for a CANDU reactor as a result of channel rupture accident with ejection of hot materials from the channel. Isles performed high-pressure melt ejection experiments related to a postulated over-power condition in the Douglas Point CANDU reactor. A 9-tube array of full-size channels was contained in a small (*i.e.*, relative to the calandria volume), open, rectangular tank. Tests were performed with and without simulated fuel bundles that were fabricated of carbon steel. The experiments were conducted at a much higher pressure (22 MPa) than the operational pressure (10 MPa) of a CANDU reactor using full size channels.

These tests were primarily designed to investigate the in-core damage caused by the high-pressure channel rupture with the melt ejection, so few quantitative measurements were taken. In some of these tests, the pressure history was recorded in the simulated moderator water in close proximity to the failed channel. These measurements show a pressure peak immediately after the channel rupture which is characteristic of the forced FCI mode due to the fine melt fragmentation within a close proximity of the rupture. Collapse of calandria tubes onto their pressure tubes is observed.

# 3.0 ANALYTICAL MODEL

The available experimental evidences, discussed in the previous section, demonstrate that the free-interaction model is unlikely to occur in the high pressure melt ejection phenomena associated with CANDU single channel events. It is more appropriate to employ the forced fuel-coolant interaction methodology in analyzing CANDU single channel severe flow blockage scenarios if some molten fuel is postulated to occur.

The forced fuel-coolant interaction methodology [9] employs several concepts and implicit assumptions. This methodology was developed using conservative assumptions such as extreme rupture conditions and a large fraction of molten fuel present at the time of rupture although single channel analyses recognize that the amount of melt present at channel rupture can only be small. The magnitudes of hydrodynamic transient loads were conservatively determined using analytical models which include bubble growth dynamics, discharge flow calculations, slug inertial behaviour, condensation at the bubble surface, impulsive loading on adjacent structures and dynamic stress analysis for the moderator tank. By considering various damage mechanisms, the integrity of the calandria vessel, adjacent fuel channels and the extent of damage to surrounding guide tubes have been evaluated.

The molten material residing immediately above the rupture opening is accelerated by the acoustic waves propagating through the molten layer and reflecting from its top surface until the steady-state discharge velocity is reached. Once the gas breaks through, the subsequent discharge is governed by the axial transport of molten material to the rupture opening. Reference [9] envelopes the range of possible discharge modes by "stratified" and "dispersed" flow models. In the stratified model, the gas and the melt travel to the rupture location at separate velocities, and mix at the rupture site. In the dispersed flow model, the gas and the melt are homogenized within the channel by the passage of an acoustic pressure wave, and the resulting mixture flows to the rupture at a common velocity.

The discharged high temperature fuel is finely fragmented, and that the molten fragments dissipate all their

stored and latent heat very rapidly. The rate at which molten and solid debris can be delivered to the moderator water to generate steam in close proximity to the break is the primary parameter in determining the ensuing hydrodynamic transient. The large amount of steam generated by the heat released from the rapid quenching process of hot fuel with cold moderator, and the discharged hydrogen gas, will form an expanding bubble.

The rate of molten fuel discharge from the fuel channel and the instantaneous pressure within the expanding steam-gas bubble can be evaluated by applying the energy balance to the expanding volume. The bubble expanding process is modelled as a spherical expansion of real gas mixture consisting of steam and hydrogen. The growth of this region is limited by the ability to push aside the surrounding liquid. To sustain this growth, a radial pressure gradient is developed in the surrounding liquid. The high moderator pressure resulting from the liquid compression produced by the expanding volume of the steam-hydrogen bubble.

The moderator pressure rises following the break and it may exceed the level required to collapse the calandria tubes onto the pressure tubes, which is about 0.6 MPa. The collapse of the calandria tubes maintains the pressure at 0.6 MPa until either the pressure decreases below this value or the available collapse volume is exhausted.

The resulting pressure gradient as well as the dynamic pressure on an adjacent structure is integrated over the exposed area to compute the hydrodynamic loadings. To determine the transmitted impulse, these loads are integrated over the transient time until the bubble and moderator pressures equalize. Then, the impulse is conservatively assumed to be wholly converted into kinetic energy in the structure, and the kinetic energy is used in evaluating the response of the adjacent structures.

Details of bubble growth, condensation, compression of water, expansion of the calandria tank and dynamic response of in-core structures are discussed in Reference [10]. The experimental support for the analytical model has been provided in Reference [9] by comparing the model predictions with the "CANDU-prototypic" experiment by Isles [8].

## 4.0 ANALYTICAL RESULTS

In this section, the models describing the thermal interactions following a postulated severe flow blockage are applied to CANDU-type of reactor channel. Following rupture of a fuel channel, hot fuel particles or droplets, gaseous hydrogen and eventually two-phase coolant are released into the moderator. In turn, this release produces strong hydrodynamic transients within the calandria vessel, which apply large loads on the in-core structures as well as the vessel itself. The models for fuel-hydrogen discharge, bubble growth, and mechanical loading of reactor structures were incorporated into a computer program. The program predicts the hydrodynamics of a severe blockage accident from the time of rupture of the pressure and calandria tubes to the dissipation of the molten fuel-hydrogen energy into the moderator. Description of the sequence of events and the magnitudes of the transients is provided below.

Although the stratified flow model, which invariably produces far more benign consequences, is more appropriate, the dispersed flow model is used for conservatism. Bounding conditions with a large fraction of molten fuel (300 kg) in the ballooned channel prior to failure is considered. The hot fuel temperature is assumed to be 2200°C. A hot gas (*i.e.*, steam and hydrogen mixture) at about 10 MPa fills the void in the channel. The rupture is initiated somewhere along the channel, and it propagates to form a crack with flow

area equal to twice the channel cross-sectional flow area. In this analysis, an idealized "fish mouth" rupture is considered. The rupture is assumed to occur with an initial crack length of 2 cm. The final length of the rip is assumed to be 0.42 m and to open in 1 ms.

It should be noted that one of the key CANDU characteristics is the ability to rapidly provide an expansion volume for the growing steam bubble in the moderator by means of calandria tubes collapse onto their pressure tubes. The volume available for the bubble expansion is higher than the conservative value of 40 percent of the available volume assumed in the calculations. The peak pressure will be limited to the calandria tube collapse pressure as long as the collapse volume is still available.

The accumulated discharged mass of hot fuel is shown in Figure 2, as a function of time. The hot fuel is completely discharged in about 135 ms. The most severe pressurization occurs within a fraction of one second following the initiation of rupture, when fine, hot fuel particles and noncondensible hydrogen are ejected at high velocities into the moderator water. The fine droplets or particles of fuel are quenched rapidly, generating large quantities of steam. The steam forms a highly pressurized and rapidly expanding bubble. Given the heat rejection transient into the moderator is quantified, the steam bubble pressure and size is readily calculated. The bubble reaches its maximum value of 1.08 m at the time of the complete discharge of the hot fuel, as indicated in Figure 3. Then the bubble starts to collapse due to the continuing condensation of steam at the bubble/liquid interface. This terminates the initial, and the most severe, pressure excursion. Subsequently, secondary pressure excursions can occur as a result of coolant discharge into the moderator, or possibly due to delayed ejection of fuel debris, if all the fuel is not ejected initially. Nevertheless, all subsequent steam bubbles will be smaller and less dynamic, resulting in much lower impulsive loads or pressure loadings on the vessel wall.

At the onset of the rupture, the bubble pressure increases rapidly, as illustrated in Figure 4, and it starts to decrease in magnitude due to the expansion of the bubble. The pressure loading on the moderator vessel wall is shown in Figure 5 for the 250 ms transient. The pressure rises to a sufficiently high level in 10 ms to begin collapsing the calandria tubes and is maintained at a plateau until the bubble reaches a diameter where condensation exceeds the rate of steam generation. At this time (~ 75 ms), the pressure decreases somewhat and the process of collapsing is interrupted. Later, the moderator pressurizes again to 0.6 MPa when the compression wave returns from the unblocked end of the fuel channel to the rupture site. This causes a step increase in the discharge velocity. After the available volume for the calandria tube collapse is consumed, the moderator pressure increases and reaches a peak at 0.85 MPa. When the fuel inventory is completely discharged, the bubble and moderator pressures decay to the ambient value (0.1 MPa).

The pressure gradient developed in the moderator to accommodate the inertial growth of the bubble could result in substantial transient pressure. The predicted pressure histories, at various distances from the rupture, are illustrated in Figure 6. The trend follows the time history of the bubble pressure and the pressure decreases in magnitude as the distance from the break increases. These pressure differences and the resulting forces would be highly transient and essentially result in impulsive loads on the structures. The time interval over which the pressure differences are generated is the time from initiation of the rupture and the formation of a high pressure bubble until the moderator pressure equilibrates with the bubble pressure. As a measure of these loads, the pressure is integrated over this time interval and shown in Figure 7. The value of the impulse per unit area decreases as the distance from the rupture site increases.

Hydrodynamic analyses were also performed to study the sensitivity of the transient to the amount of fuel available for discharge. Three values of the discharged fuel mass are considered, namely 300, 200 and 100

kg. The results are also compared with the case where no fuel is discharged. The accumulated discharged fuel mass is shown in Figure 8, as a function of time. The fuel is completely discharged within the first 135, 105 and 60 ms for 300, 200 and 100 kg cases, respectively. Therefore, the three cases are identical within the period of 60 ms following the initiation of rupture. The bubble reaches its maximum value at the time of the complete discharge of the hot fuel, as indicated in Figure 9. For the case of no discharged fuel, the bubble formation is due to the hot mixture of ejected gases and the bubble radius is smaller in comparison with the other cases.

At the onset of the rupture, the bubble pressure increases rapidly, as illustrated in Figure 10, and it starts to decrease in magnitude due to the expansion of the bubble, in all cases. When the fuel inventory is completely discharged, the bubble decays to the ambient value (0.1 MPa). This explains the disappearance of the third peak in the cases of 200 and 100 kg discharged fuel.

The pressure loading on the moderator vessel wall is shown in Figure 11. For the case of no discharged fuel, the pressure increases rapidly to about 0.5 MPa, and then starts to decrease gradually. For other cases, the pressure rises following the channel failure, and exceeds the level required to collapse the calandria tubes onto the pressure tubes, which is about 0.6 MPa. The collapse of the calandria tubes maintains the pressure at 0.6 MPa until either the pressure decreases below this value (e.g., fuel discharging into the moderator is exhausted, such as in the cases of 200 and 100 kg) or the available volume for collapsing is exhausted and the pressure peaks again (such as in the case of 300 kg).

In all cases, the value of the impulse per unit area decreases as the distance from the rupture site increases, as shown in Figure 12. The magnitude of the loading depends upon the amount of fuel discharged. The higher discharged mass produces more energy deposited in the bubble over the transient which results in a faster and greater pressurization of the moderator and results in higher impulsive loads on adjacent structures.

## 5.0 CONCLUSIONS

The modelling of fuel-coolant interaction following a severe power-cooling mismatch in a single channel of a CANDU reactor is assessed. The forced interaction model postulates that the melt is ejected from the channel at sufficiently high velocities to be finely fragmented and rapidly quenched within milliseconds of the ejection. The hydrodynamic transient characterized by forced interaction displays a pressure transient occurring immediately after the rupture and continues throughout the blowdown of the melt. The free interaction model postulates that the melt is ejected at low velocities and accumulates outside of the channel as a coarse melt-water-steam mixture. Some time later, this coarse mixture is triggered to finely fragments and rapidly quenches. The hydrodynamic transient characterized by free interaction model displays a delayed FCI occurring after the end of the molten pour, resulting in a larger and shorter, in duration, pressure spike.

The available data that support these models are also reviewed. It is concluded that the free-interaction model is not suited for the high pressure melt ejection phenomena associated with CANDU single channel events. It is appropriate to employ the forced fuel-coolant interaction methodology in analyzing CANDU single channel flow blockage event with a severe power-cooling mismatch. The forced fuel-coolant interaction is always energetic in nature (*i.e.*, it always generates shock loads). The initial hydrodynamic transient and the damage potential are generally dependent on the discharge rate of the melt from the channel.

It should be noted that melt pools could exist in the channel (in the case of a flow blockage scenario) only if the pressure tube failure mechanisms are conservatively ignored. Therefore, it is recommended to quantify the circumferential temperature gradient of the pressure tube under full system pressure and assess potential for failure of the pressure tube due to circumferential temperature gradients and to quantify the amount of molten fuel and its deposition at the time of channel failure.

The magnitudes of hydrodynamic transient loads were conservatively determined using analytical models which include bubble growth dynamics, discharge flow calculations, slug inertial behaviour, condensation at the bubble surface, impulsive loading on adjacent structures and dynamic stress analysis for the moderator tank. The most severe pressurization occurs within a fraction of one second following the initiation of rupture, when fine, hot fuel particles and noncondensible hydrogen are ejected at high velocities into the moderator water.

The pressure loading on the moderator vessel wall rises following the channel failure, and may exceed the level required to collapse the calandria tubes onto the pressure tubes, which is about 0.6 MPa. The collapse of the calandria tubes maintains the pressure at 0.6 MPa until either the pressure decreases below this value (e.g., fuel discharging into the moderator is exhausted) or the available volume for collapsing is exhausted and the pressure peaks again.

The magnitude of the pressure transient and impulse per unit area decrease as the distance from the rupture site increases. Also, the higher discharged mass produces more energy deposited in the bubble over the transient which results in a faster and greater pressurization of the moderator and results in higher impulsive loads on adjacent structures.

## 6.0 REFERENCES


[1] J.H.K. Lau and C. Blahnik, "Consequences of Flow Blockage in a CANDU Fuel Channel Under Full Power Operation", Ontario Hydro Report No. 84042, March, 1984.

[2] M.L.Corradini, "Direct Containment Heating", Fission Product Transport Processes in Reactor Accidents, Edited by J.T.Rogers, 1990.

[3] W.W. Tarbell et al., "Pressurized Melt Ejection into Water Pools", NUREG/CR-3916, March 1991.

[4] M.D.Allen et al., "Experiments to Investigate the Effects of Flight Path on Direct Containment Heating (DCH) in the Surtsey Test Facility ", NUREG/CR-5728, 1991.

[5] M.D.Allen et al., "Experiments to Investigate the Effects of Water in the Cavity on Direct Containment Heating (DCH) in the Surtsey Test Facility ", SAND91-1173, 1992.

[6] M.D.Allen et al., "Experiments to Investigate the Effects of Fuel/Coolant Interactions on Direct Containment Heating ", SAND92-2849, 1993.

[7] T. Fuketa and T. Fujishiro, "Generation of Destructive Forces During Fuel/Coolant Interactions Under Severe Reactivity Initiated Accident Conditions", Nuclear Engineering and Design, 146, p. 181-194, 1994.

[8] R. Isles, "Lattice Site Shock Test", TDVI-95, AECL, December 1965.

[9] Fauske & Associates, "Analyses of Thermal Interactions Following the Hypothetical Severe Blockage of a Coolant Channel", Report FAI/83-15, December 1983, (Attached as Appendix G in Reference 1).

[10] R.E.Henry, "An Assessment of a Fuel Channel Rupture within a Calandria Tank in CANDU Reactors", 5th International Conference on Nuclear Engineering, May 1997, Nice, France.

**TABLE 1**

**INITIAL CONDITIONS FOR THE INTEGRAL EFFECTS TESTS**

| | IET-1 | IET-7 | IET-8A | IET-8B |
|---|---|---|---|---|
| Mass of initial thermite (kg) | 43.0 | 43.0 | 43.0 | 43.0 |
| Cavity water (kg) | 3.48 | 3.48 | 62.0 | 62.0 |
| Gas pressure at failure (MPa) | 7.10 | 7.10 | 1.60 | 6.25 |

**FIGURE 1: COMPARISON OF THE CAVITY PRESSURES VERSUS TIME**

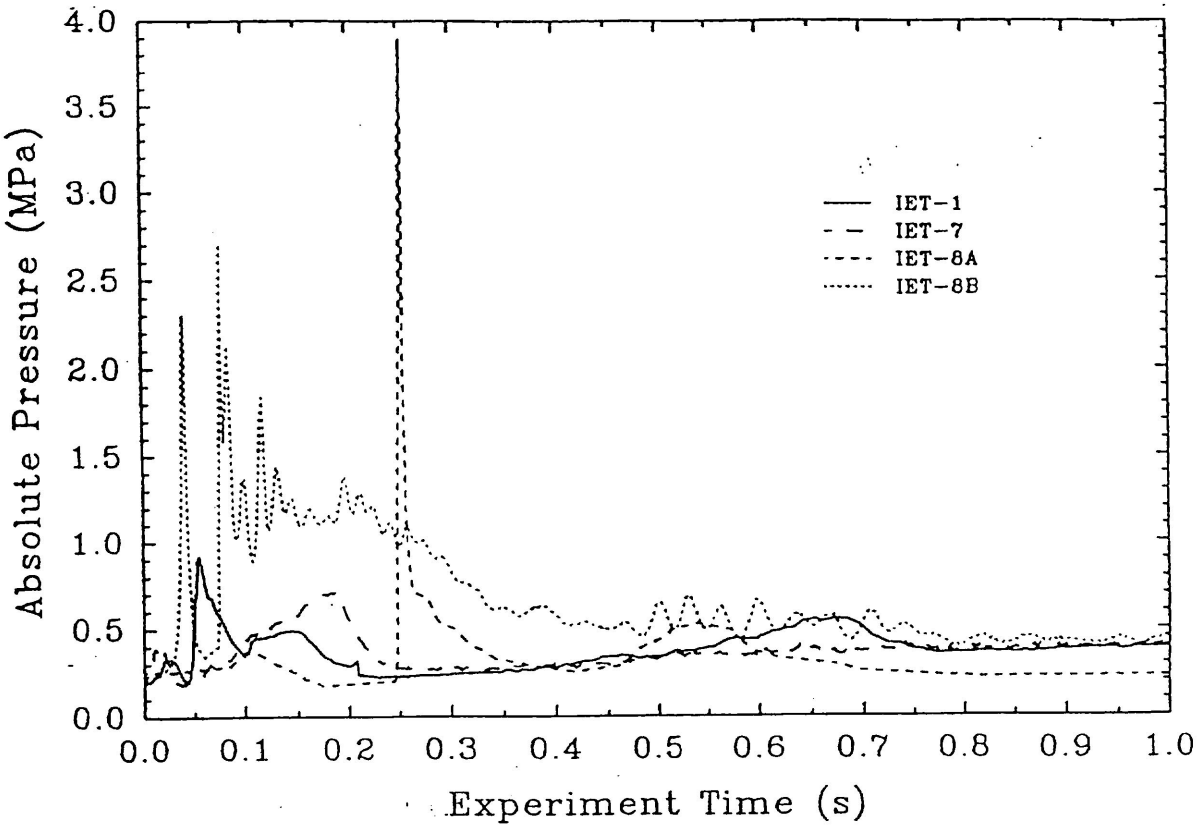


**FIGURE 2: ACCUMULATED DISCHARGED MASS VERSUS TIME**

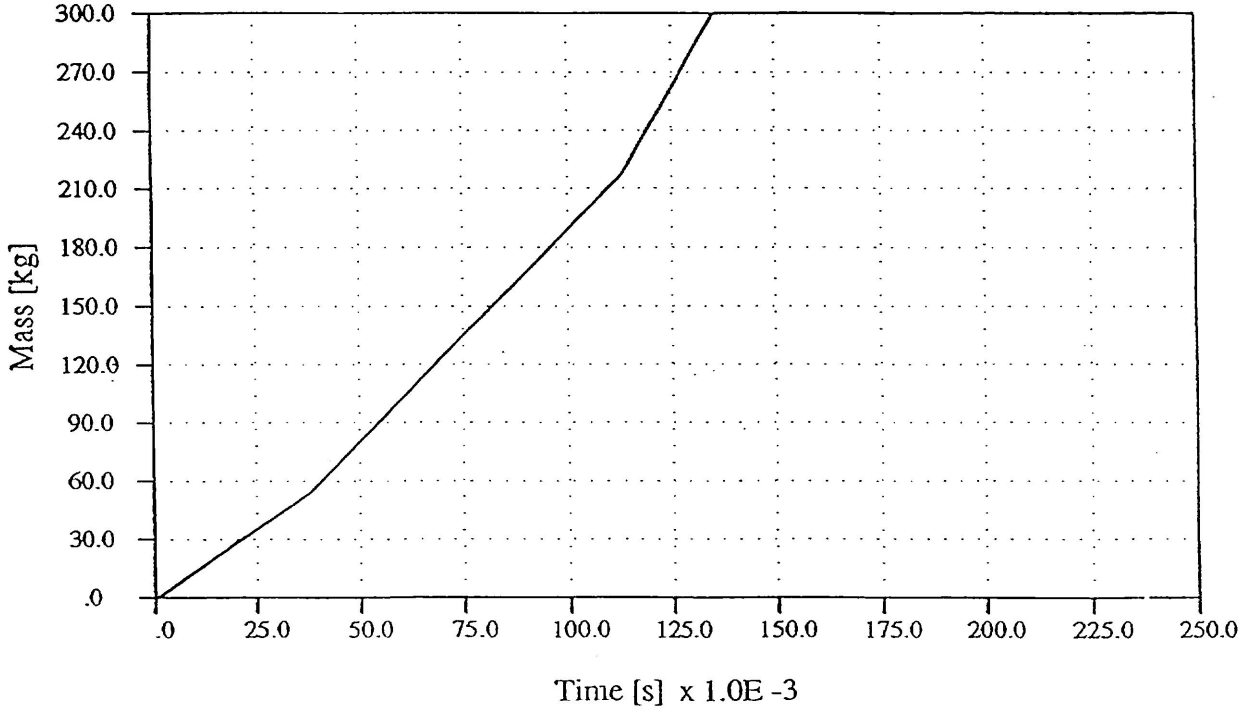


Fri Feb 28 18:32:53 1997
nwhbx/miske_jmp/gen-plot

**FIGURE 3: BUBBLE RADIUS VERSUS TIME**

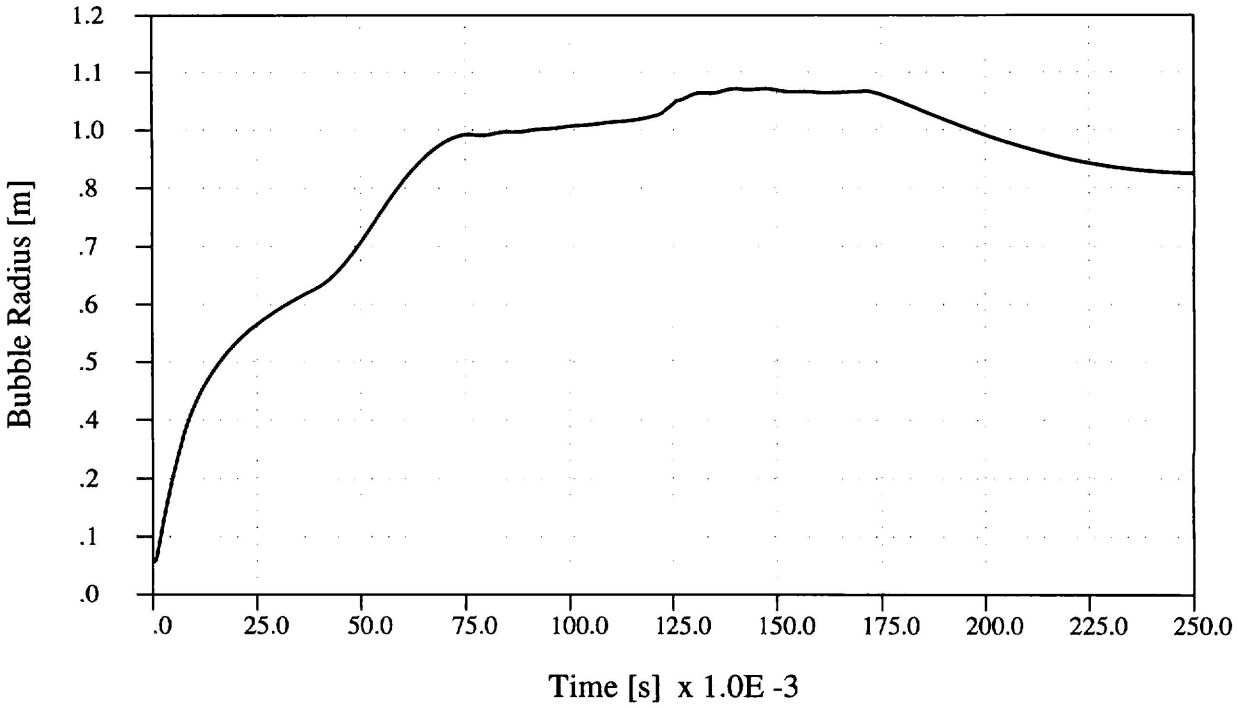


**FIGURE 4: BUBBLE PRESSURE TRANSIENT**

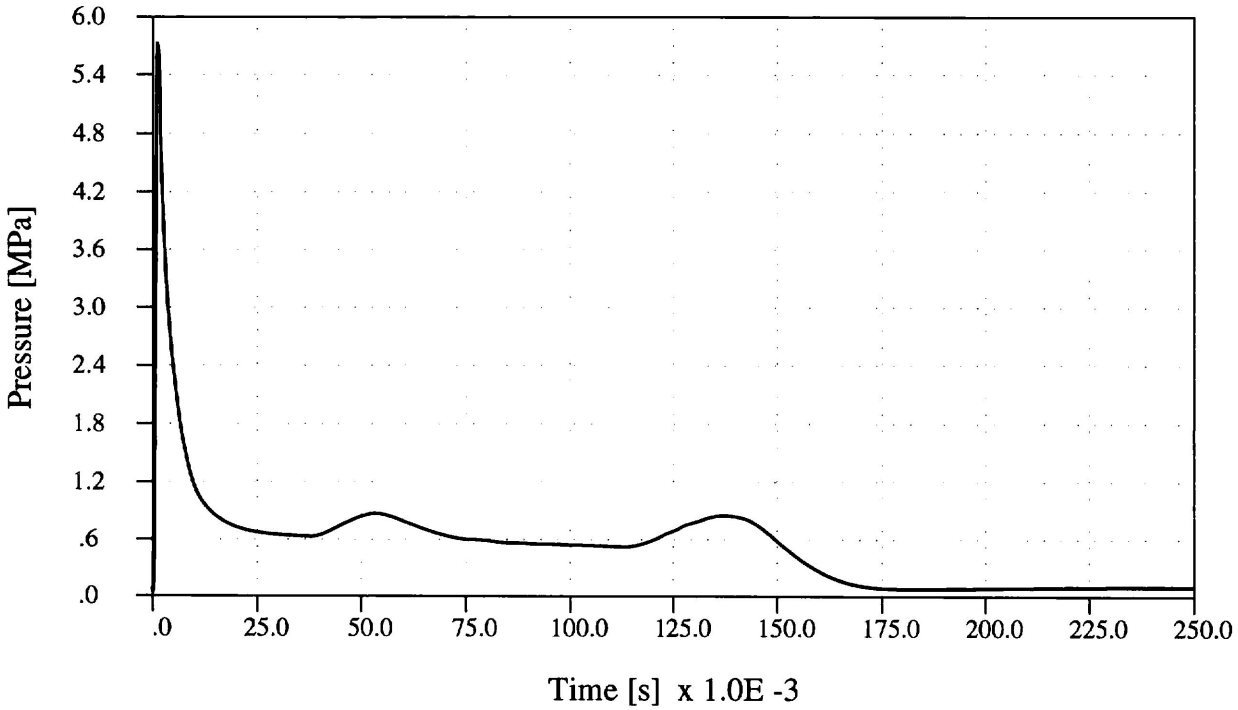


Fri Feb 28 18:32:53 1997
mwahba/fauske_pap/gen-plot

**FIGURE 5: PRESSURE TRANSIENT ON CALANDRIA VESSEL WALL**

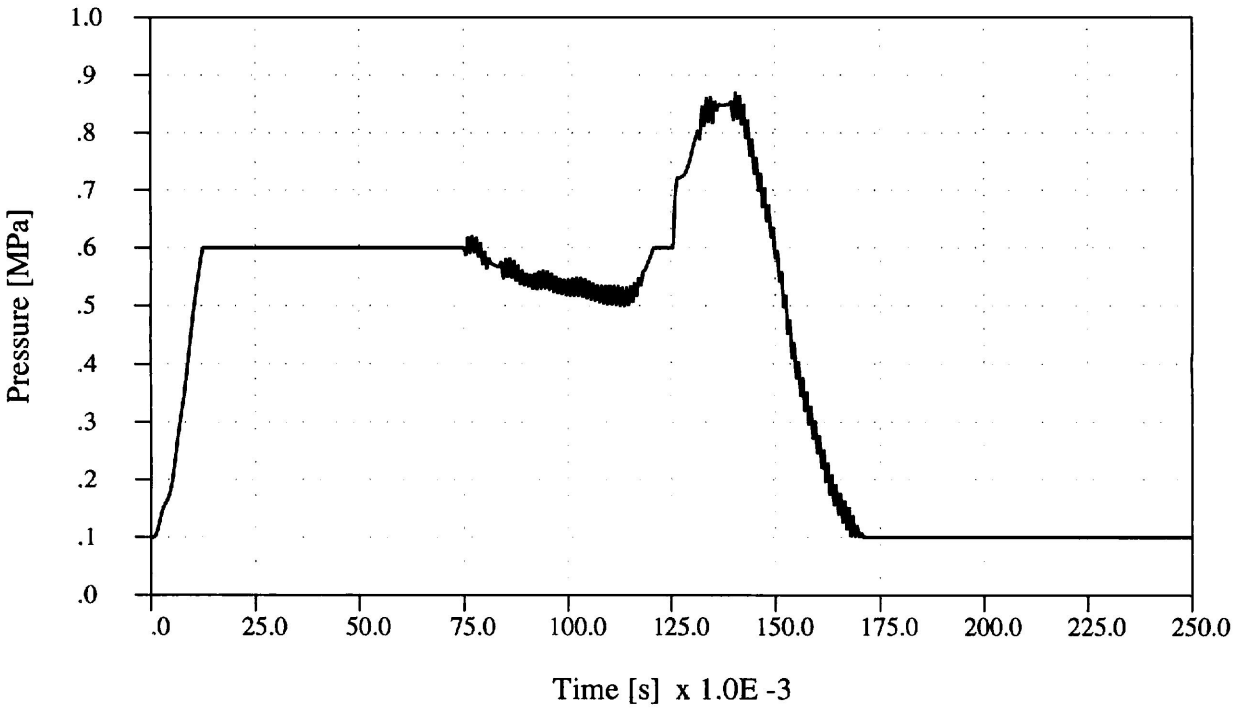


**FIGURE 6: MODERATOR PRESSURE TRANSIENT AT VARIOUS LOCATIONS**

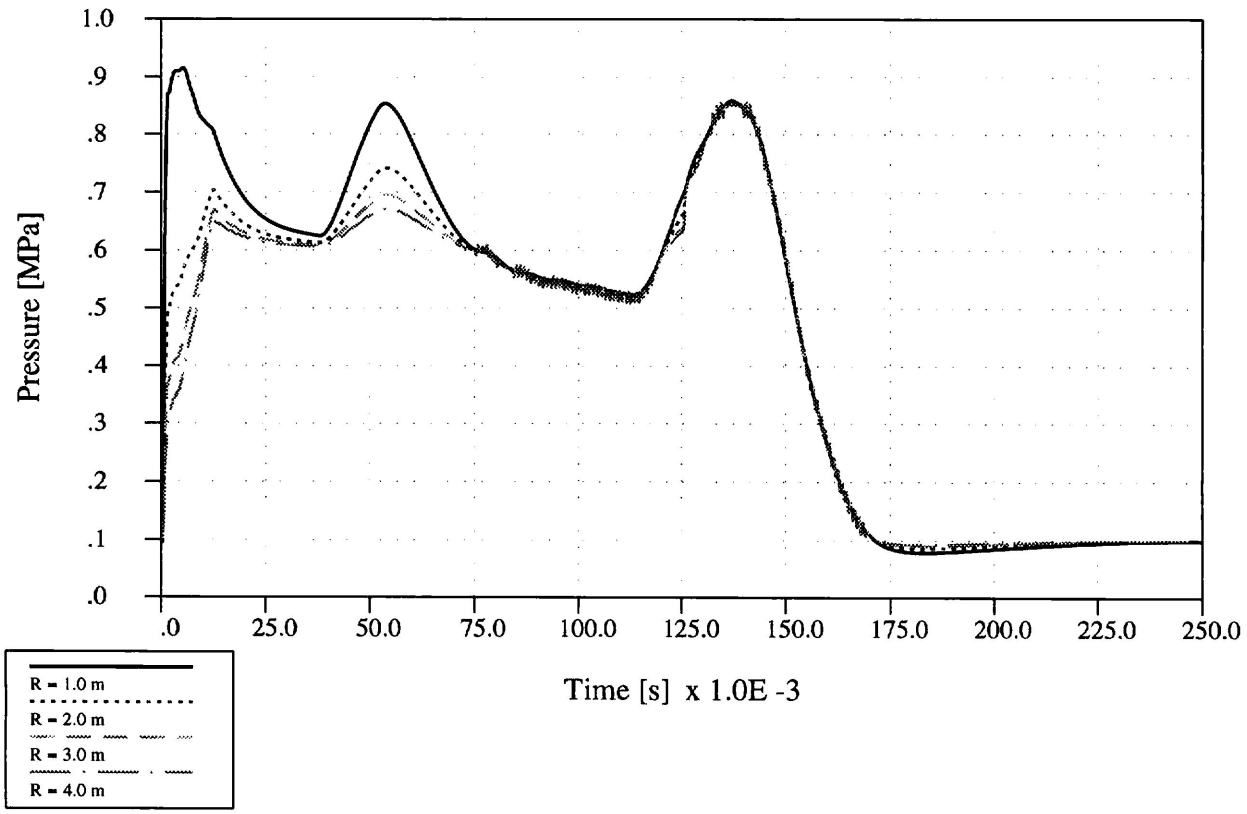

**FIGURE 7: IMPULSE PER UNIT AREA VERSUS DISTANCE**

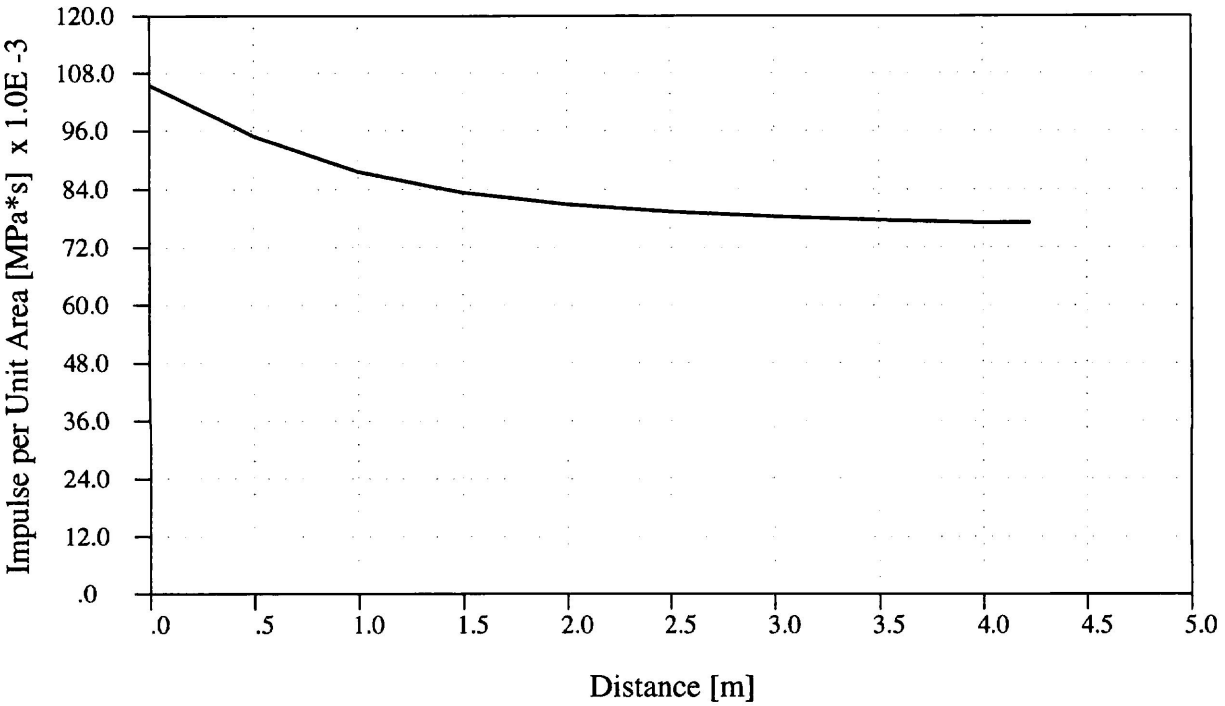


**FIGURE 8: ACCUMULATED DISCHARGED MASS VERSUS TIME FOR VARIOUS EJECTED MASS**

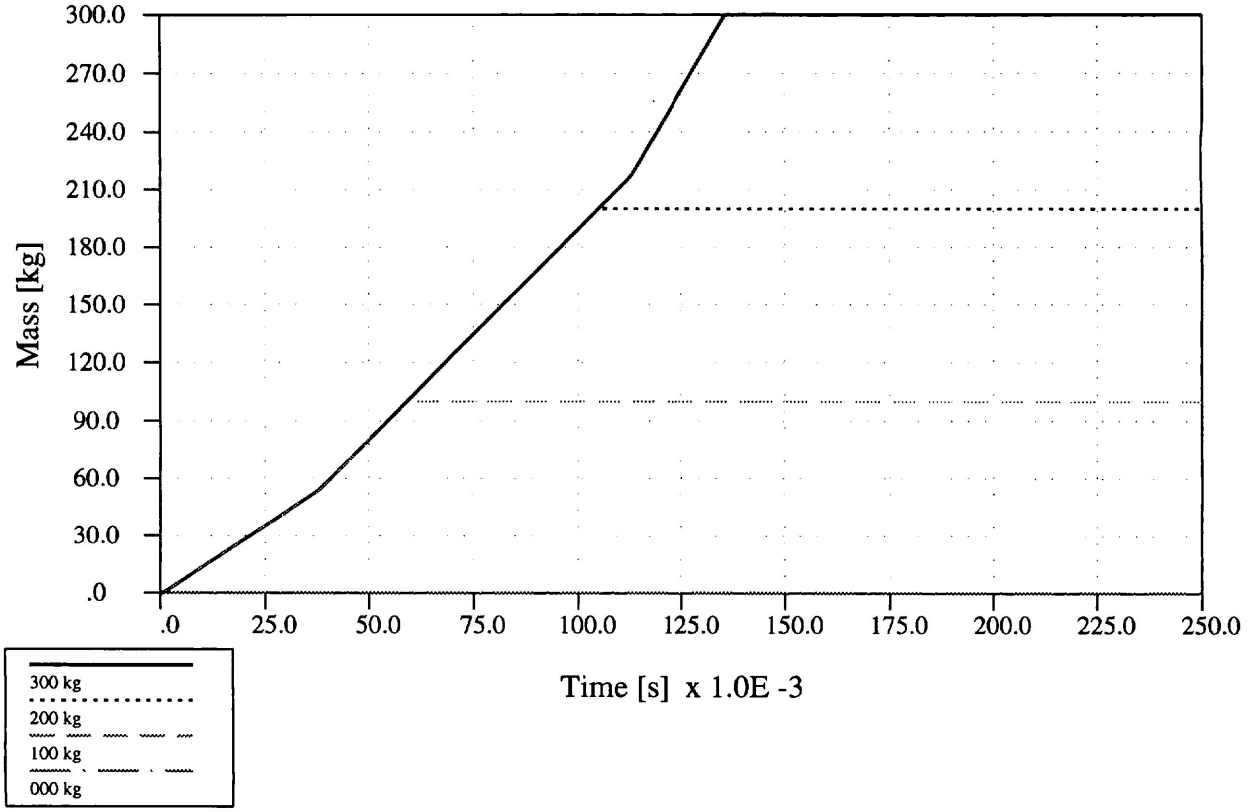


Fri Feb 28 18:32:53 1997
mwahba/fauske_pap/gen-plot

**FIGURE 9: BUBBLE RADIUS VERSUS TIME FOR VARIOUS EJECTED MASS**

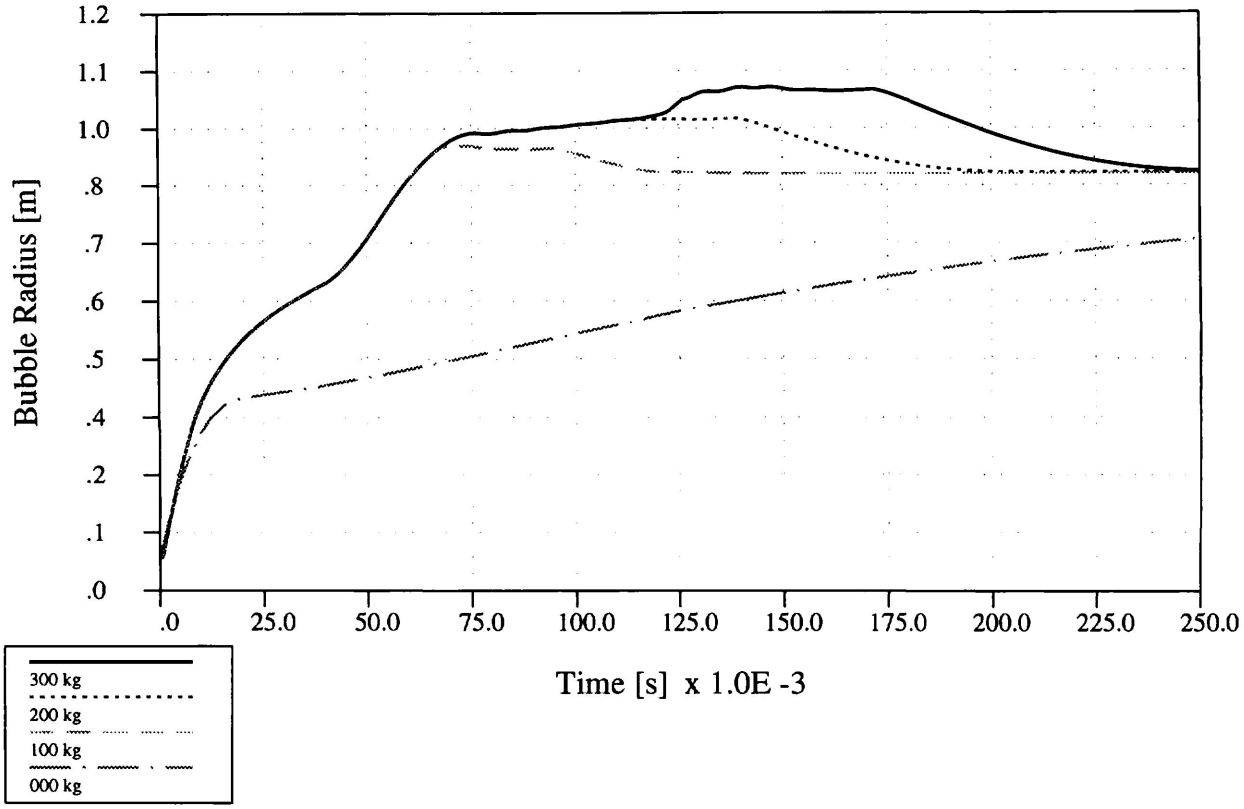


**FIGURE 10: BUBBLE PRESSURE TRANSIENT FOR VARIOUS EJECTED MASS**

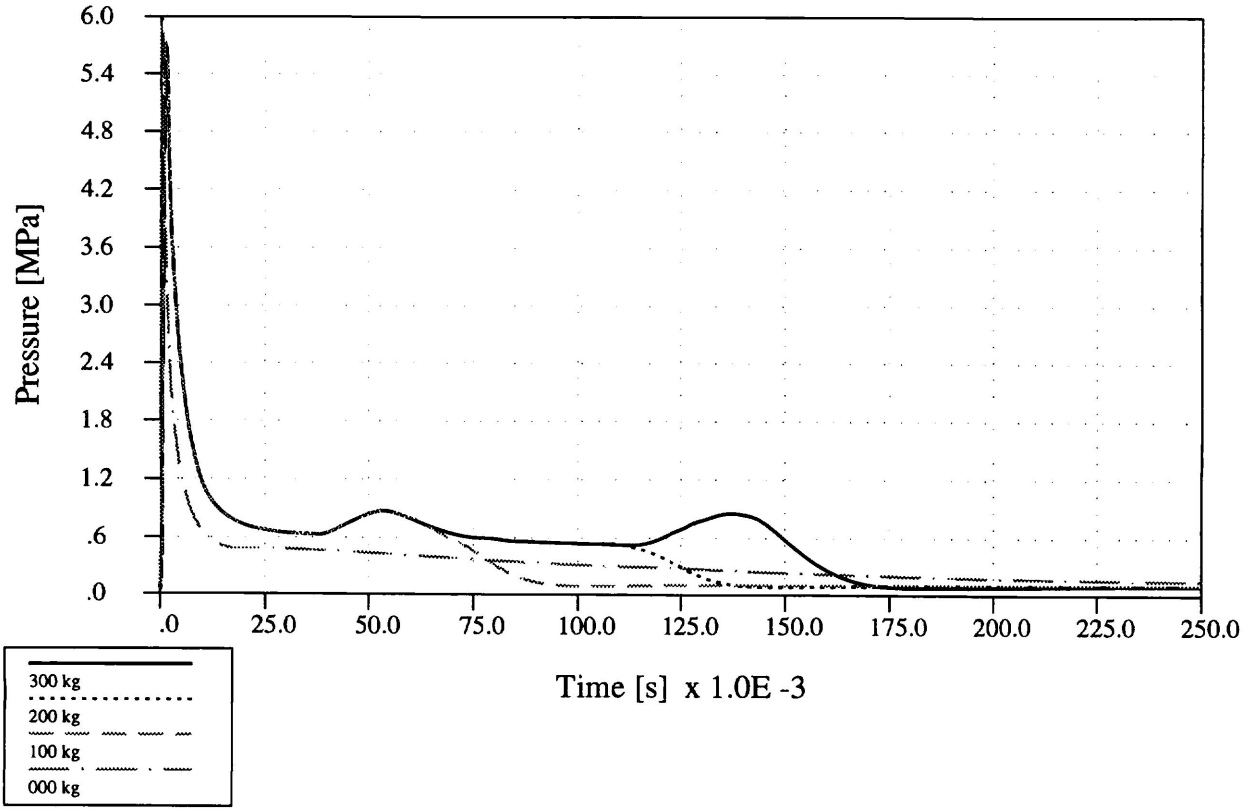


Fri Feb 28 18:32:53 1997
mwahba/fauske_pap/gen-plot

**FIGURE 11: PRESSURE TRANSIENT ON CALANDRIA VESSEL WALL FOR VARIOUS EJECTED MASS**

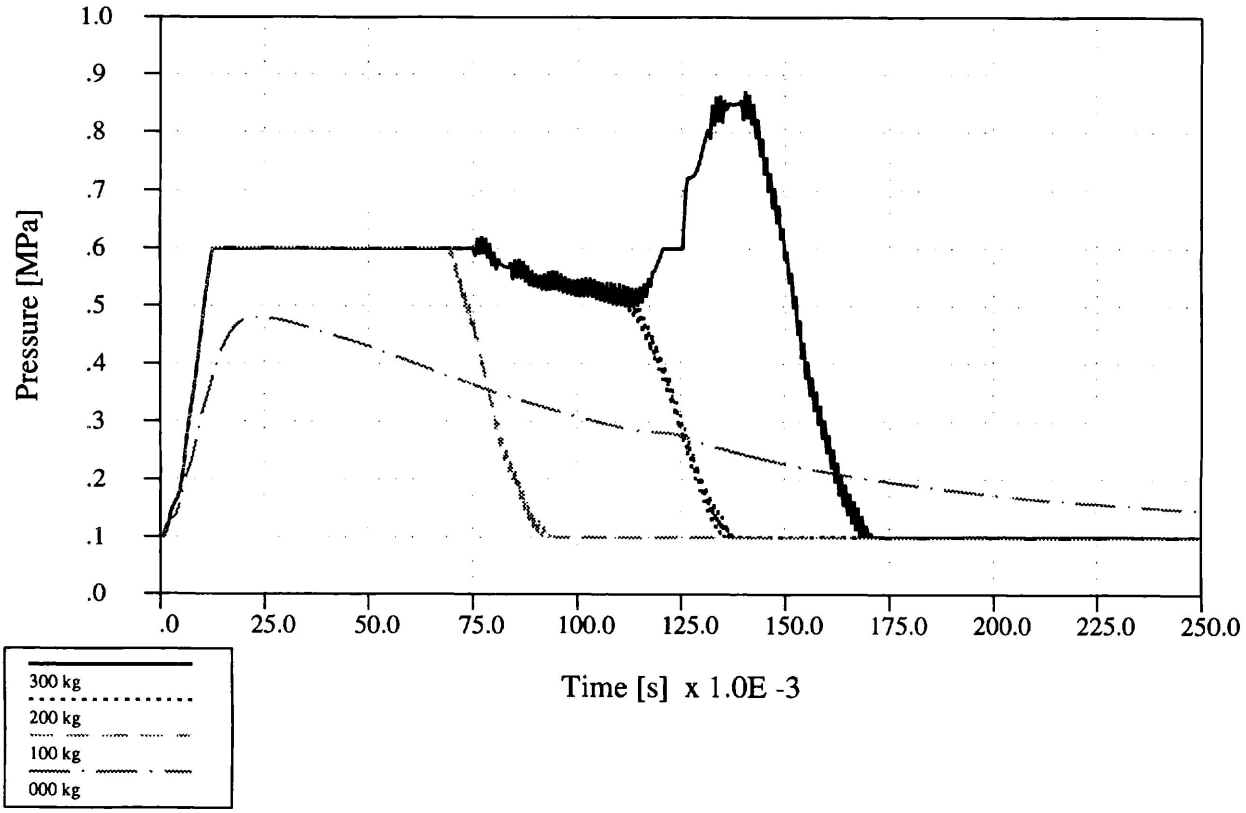


**FIGURE 12: IMPULSE PER UNIT AREA VERSUS DISTANCE FOR VARIOUS EJECTED MASS**

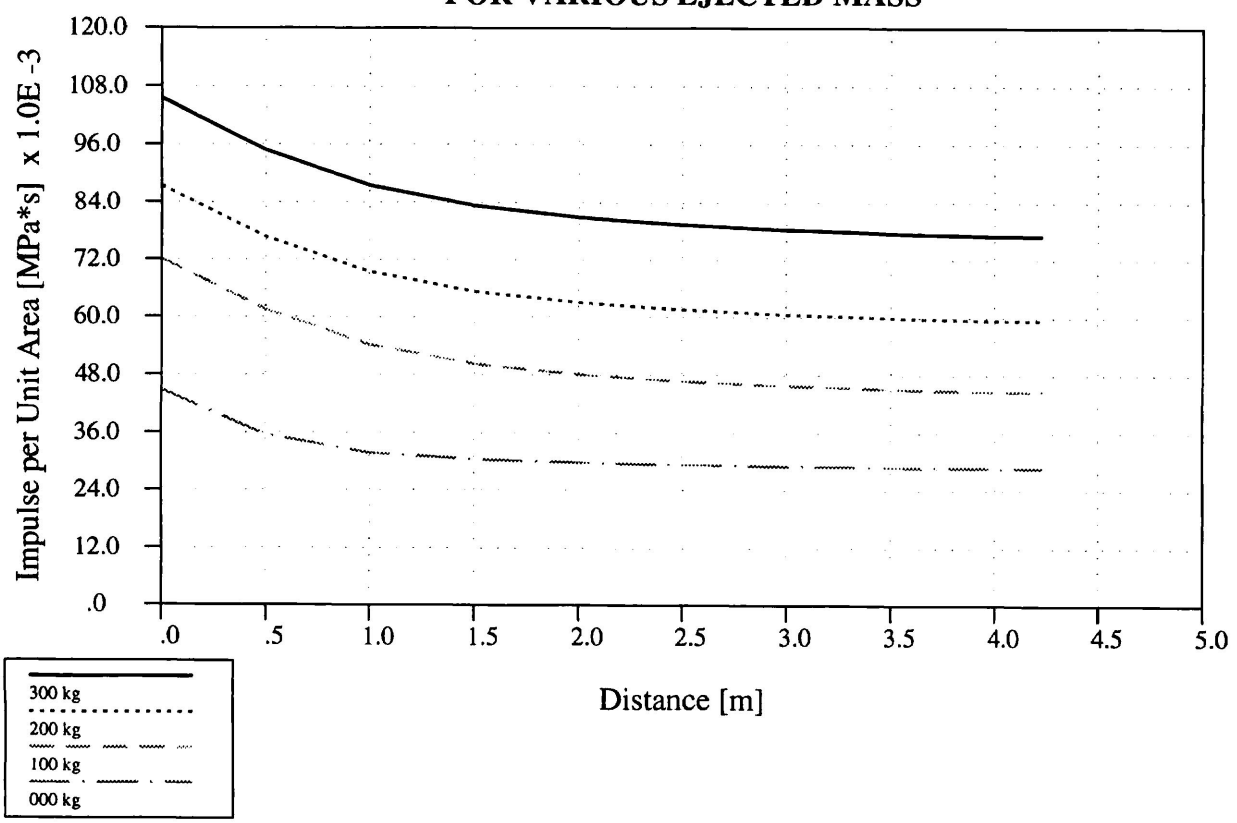


Fri Feb 28 18:32:53 1997
nwahbe/fauske_pap/gen-plot